Gas-phase decomposition of formic acid over α-Fe_2O_3 catalysts

Samih A. Halawy [a,*], Shar S. Al-Shihry [a] and Mohamed A. Mohamed [b]

[a] *Department of Chemistry, College of Education, King Faisal University, PO Box 1759, Hofuf 31982, Eastern Province, Saudi Arabia*

[b] *Department of Chemistry, Faculty of Science, South Valley University, Qena 83511, Egypt*

Received 20 March 1997; accepted 12 August 1997

α-Fe_2O_3 catalyst samples were used for the decomposition of formic acid, in the gas phase. These catalysts were produced by calcination of $Fe(NO_3)_3 \cdot 9H_2O$ for 5 h, in air, in the temperature range 200–600°C. All catalysts were characterized by temperature-programmed reduction (TPR) and X-ray diffraction (XRD). In addition, the surface area (S_{BET}) of these samples as well as the acidity and the basicity were determined. The catalytic gas-phase decomposition of formic acid was studied over α-Fe_2O_3 samples, at 200°C, in a flow system. Carbon monoxide, carbon dioxide and formaldehyde were identified as the decomposition products using gas chromatography. A correlation between the acid–base characters of the used catalysts, and the rate of the decomposition products has been made. Also, a reaction mechanism is discussed.

Keywords: acidity, basicity, catalysis, decomposition, α-Fe_2O_3, formic acid, surface area, thermal analysis, TPR, XRD

1. Introduction

The catalytic decomposition of a number of aliphatic carboxylic acids has been extensively studied [1–5]. Among these, formic acid was used in several studies to investigate the dehydrogenation and dehydration power of some catalysts [6,7]. King et al. [8] studied the catalytic decomposition of formic acid, in aqueous phase, in the presence of some nobel metal chlorides as catalysts. Some other articles have dealt with the adsorption and desorption of formic acid over metal surfaces [9–11]. Iron oxides are known to be good catalysts for oxidation of methanol [12], benzoic acid [13], the selective reduction of acetic acid [4,5], the removal of hydrogen sulfide from town gas [14] and the conversion of CO_2 into methane [15]. The preparation of α-Fe_2O_3 from different precursors [16,17] and its characterization using different techniques have been reported [18,19].

The present work concerns with the catalytic gas-phase decomposition of formic acid using α-Fe_2O_3. An attempt is made to correlate the acid–base characters of these catalysts and the rate of formation of the decomposition products of formic acid.

2. Experimental

2.1. Materials and techniques

α-Fe_2O_3 samples were prepared via calcination of $Fe(NO_3)_3 \cdot 9H_2O$ (Hopkin & Williams) in air, for 5 h, in the temperature range 200–600°C.

Thermogravimetric analysis (TGA) and differential thermal analysis (DTA) of ferric nitrate (FN) were performed using a thermobalance type Li160 KS Netzsch Gerätebau GmbH Selb (Germany) from ambient to 500°C. Heating rate of 5°C min^{-1} and a dynamic atmosphere of air (40 cm^3 min^{-1}) were applied. Highly sintered α-Al_2O_3 was the thermally inert reference material used in the DTA measurements.

X-ray diffraction measurements were performed using a Philips powder diffractometer mounted on a Philips PW-2103/00 X-ray generator with Ni-filtered Cu Kα radiation ($\lambda = 1.542$ Å).

Surface areas (S_{BET}) of α-Fe_2O_3 samples were determined on a Carlo-Erba, single-point, SORPTY 1750 unit by the conventional BET method using N_2 as adsorbate at −196°C.

The TPR apparatus used for the temperature-programmed reduction of Fe_2O_3 samples has been described elsewhere [20]. TPR profiles were recorded with ~ 10 mg, sample weight, and the H_2 consumption was monitored while the sample was heated from ambient to 800°C in a stream of 6% H_2/N_2 (40 cm^3 min^{-1}).

The acidity (Ψ) and the basicity (Φ) of the oxide samples were estimated thermogravimetrically, as described previously [21], using the adsorption of pyridine and formic acid, respectively, as probe molecules. The weight loss, due to the desorption of pyridine and formic acid from the acidic and basic sites, was determined as a function of both the acidity or the basicity of these oxides. Values of Ψ and Φ were expressed as mol sites m_{cat}^{-2} [22,23].

* Permanent address: Department of Chemistry, Faculty of Science, South Valley University, Qena 83511, Egypt. E-mail: IN%"svalleyu@FRCU.EUN.EG".

2.2. Reactivity studies

Measurements of activity and selectivity of the calcination products of ferric nitrate during the decomposition course of HCO_2H were conducted at atmospheric pressure in a continuous flow mode, using a mixture of 1.73% HCO_2H in dry N_2, obtained by passing N_2 through liquid HCO_2H in a saturator at 5°C. The total feed flow-rate 41.3 cm^3(STP) min^{-1} was composed of 0.7 cm^3(STP) min^{-1} HCO_2H and 40.6 cm^3(STP) min^{-1} dry N_2 . A catalyst sample of 100 mg was stabilized in a pyrex glass reactor for 1 h at 180°C before measurements. The reactor effluent was analyzed by a gas chromatograph (Shimadzu GC-14A) equipped with a data processor model Shimadzu Chromatopac C-R4AD (Japan), TCD and SUS, PEG 6000 10% on Shimalite TPA, 60/80 mesh (3 mm i.d. × 2 m) column at 140°C. Automatic sampling was performed with a heated gas sample cock, type HGS-2. The retention time of formic acid, as a reactant, and the expected decomposition products (i.e. CO, CO_2 and HCHO) has been calibrated in separate experiments using pure analytical grade materials.

The %conversion, selectivity to each product and the reaction rates during the decomposition of HCO_2H were calculated as explained in detail previously [24,25].

3. Results and discussion

3.1. Characterization of catalysts

3.1.1. Thermal analysis

TG and DTA curves of $Fe(NO_3)_3 \cdot 9H_2O$ are shown in figure 1. The TG curve shows a somewhat fast decomposition which results in the overlap of both the dehydration and the decomposition steps. The product Fe_2O_3 is formed at about 300°C [26], see TG curve. The DTA curve of FN (figure 1) exhibits three endothermic peaks at $T_{max} = 101$°C due to dehydration and at 156.5 and 220°C, with a small shoulder at 203°C, attributed to the decomposition [27] and the evolution of final traces of nitrogen oxides.

3.1.2. X-ray diffraction analysis

Figure 2 shows the XRD diffractograms of the calcination products of FN at different temperatures. None of the diffraction lines of the calcination products at 200°C, figure 2a, belong to Fe_2O_3. Increasing the calcination temperature to 300°C has resulted in the formation of a well defined α-Fe_2O_3 lattice structure, figure 2b. The degree of crystallinity increases as the calcination temperature increases up to 600°C. This is indicated by the values of the d-spacings that match the characteristic lines at $d = 3.73$, 2.70, 2.51, 2.21, 1.84 and 1.69 Å of hematite α-Fe_2O_3, ASTM card No. 24-72 A.

3.1.3. Temperature-programmed reduction (TPR)

The typical reduction profiles of FN samples are presented in figure 3. The TPR profiles of FN calcined at 200°C (figure 3a) show three reduction peaks with T_{max} at 259, 335 and 524°C. The first peak located at 259°C may be due to the reduction of the residual undecomposed nitrate in this sample (see TG curve, figure 1), while the other two peaks at 335 and 524°C correspond

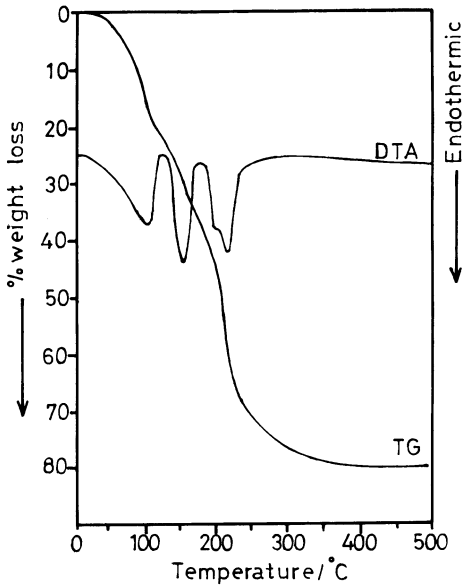

Figure 1. TG and DTA curves of $Fe(NO_3)_3 \cdot 9H_2O$ carried out at 5°C min^{-1} in a dynamic atmosphere of air (40 cm^3 min^{-1}).

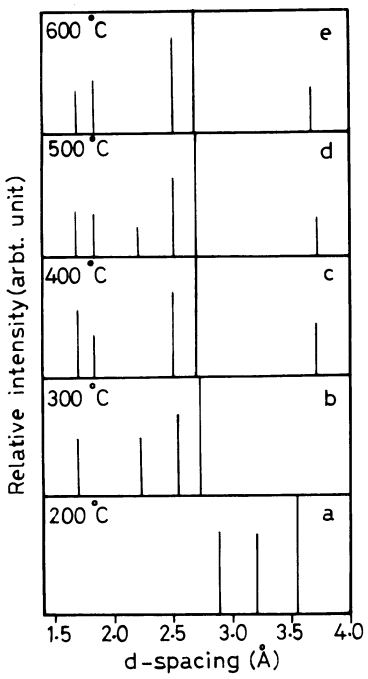

Figure 2. XRD patterns of the calcination products of $Fe(NO_3)_3 \cdot 9H_2O$ at different temperatures, for 5 h in air.

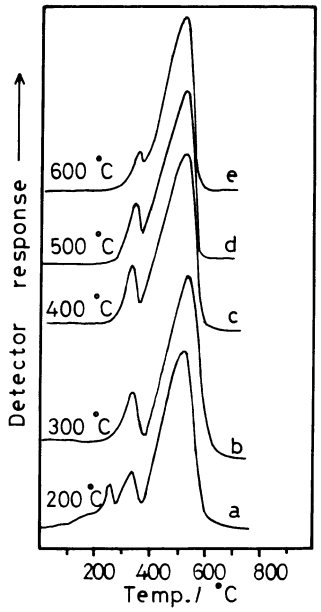

Figure 3. TPR profiles of the calcination products of $Fe(NO_3)_3 \cdot 9H_2O$ at different temperatures, for 5 h in air.

to the stepwise reduction of α-Fe_2O_3 to metallic Fe [28] as follows:

$$\alpha\text{-}Fe_2O_3 \text{ (hematite)} \rightarrow Fe_3O_4\text{(magnetite)} \rightarrow Fe \text{ (metal)}$$

This is consistent with a previously published mechanism [29], where no FeO (wüstite) is formed below 575°C. The rest of the TPR profiles (b–e) showed only two peaks. The first peak varied between 335 and 360°C, while the second peak in the range 531–549°C. The amount of hydrogen that is required for the complete reduction of Fe_2O_3 is calculated theoretically [30] as 1.87×10^{-2} mol g^{-1}. This value is in good agreement with the H_2 uptake found practically (see table 1). Also, evidence for the formation of Fe_3O_4 as an intermediate in the reduction process of α-Fe_2O_3 has been given previously by Gazzarini and Lanzavecchia [31].

Samples calcined in the temperature range 300–600°C have shown nearly the same amount of H_2 uptake (i.e. 1.94×10^{-2} mol g^{-1}). TPR results are parallel with those of TG and XRD analyses where α-Fe_2O_3 is clearly formed by calcination of FN at temperatures $\geqslant 300$°C.

3.2. Reactivity measurements

The activity of a catalyst is known to depend on the concentration of active sites, per unit weight (or surface area) of that catalyst and, also, the types of these active sites. α-Fe_2O_3 has been shown [32,33] to possess both surface Brønsted acidic and basic sites where the Brønsted basic sites were, relatively, higher than the acidic sites [24].

A summary of the characteristics of the catalytic decomposition of formic acid over the calcination products of $Fe(NO_3)_3 \cdot 9H_2O$ at different temperatures is given in figure 4 and table 1.

3.2.1. Effect of calcination temperature on the %conversion and the surface area (S_{BET})

Figure 4 shows that %conversion decreases sharply with increasing the calcination temperature at first (between 200 and 400°C), then it decreases slightly above 400°C. For example, the sample calcined at 200°C was shown to possess the highest value of %conversion (ca. 24.1%). As the calcination temperature increases to 400°C, the %conversion has decreased to 10.3% (i.e. less than half of that measured for the catalyst calcined at 200°C). Above 400°C, however, the %conversion continued to decrease slightly to 10.3 and 8.6% for catalysts calcined at 500 and 600°C, respectively.

Table 1 shows that the surface area (S_{BET}) is inversely proportional to the calcination temperature of these samples, i.e. a behavior which is exactly parallel to the %conversion.

Three gaseous products were detected by GC analysis during the decomposition course of HCO_2H and were identified as CO, CO_2 and formaldehyde HCHO. Each of these compounds represents a product of different chemical process.

(i) Dehydration process (i.e. $HCO_2H \rightarrow CO + H_2O$). A small concentration of carbon monoxide (CO) as a result of the dehydration process of formic acid [7] was

Table 1
S_{BET}, acidity–basicity, H_2-uptake and kinetic parameters of the gas-phase catalytic decomposition of formic acid over the calcination products of $Fe(NO_3)_3 \cdot 9H_2O$, at different temperatures for 5 h in air [a]

Calcin. temp. (°C)	S_{BET} ($m^2\ g^{-1}$)	H_2-uptake ($\times 10^{-2}$ mol g^{-1})	Acidity [b] Ψ	Basicity [b] Φ	%Conv.	%Selectivity		
						$\%S_{CO_2}$	$\%S_{CO}$	$\%S_{HCHO}$
200	47.9	2.06	1.29×10^{18}	14.86×10^{18}	24.1	83.4	12.0	4.6
300	30.1	1.94	0.47×10^{18}	19.50×10^{18}	14.8	60.8	18.8	20.4
400	22.2	1.93	0.63×10^{18}	17.21×10^{18}	10.3	58.2	22.6	19.2
500	21.8	1.93	0.55×10^{18}	9.49×10^{18}	9.0	59.7	23.9	16.3
600	10.7	1.93	0.62×10^{18}	7.76×10^{18}	8.6	58.6	24.9	16.5

[a] %reactant = 1.73, $W/F = 0.91\ g_{cat}$ mol ℓ^{-1} h^{-1}, total flow rate = 41.3 cm^3(STP) min^{-1}, reaction temperature = 200°C.
[b] mol sites m_{cat}^{-2}.

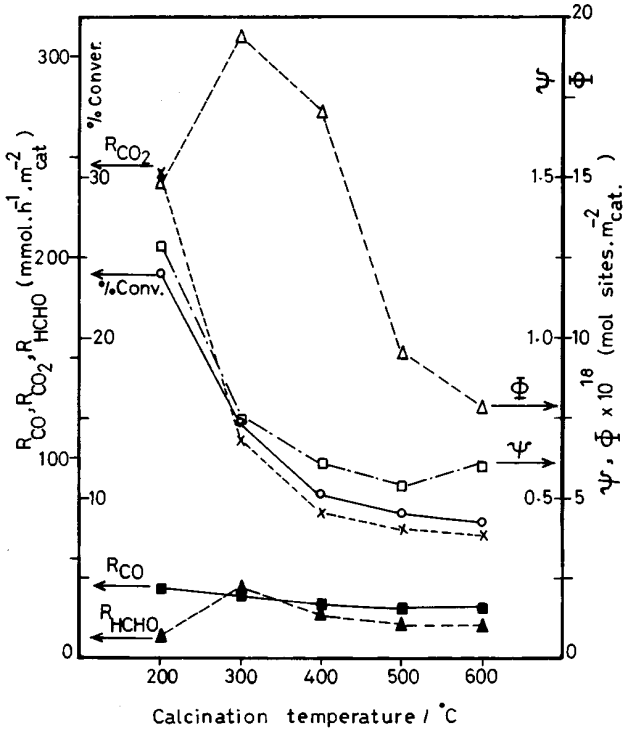

Figure 4. The relationship between the acid–base characters and the activity of α-Fe_2O_3, prepared at different temperatures, during the catalytic decomposition of HCO_2H.

always less than the concentration of the other two gaseous products. The catalyst calcined at 200°C showed the maximum rate of formation of CO (R_{CO}), ca. 34.9 mmol h^{-1} m^{-2}_{cat}, and possessed, also, the maximum concentration of the surface acidic sites ($\Psi = 1.29 \times 10^{18}$ mol sites m^{-2}_{cat}). As the calcination temperature increases both R_{CO} and the acidity values Ψ of these catalysts decrease gradually. The acidity values for the last three catalysts, calcined between 400 and 600°C, were nearly constant (i.e. 0.6×10^{18} mol sites m^{-2}_{cat}). The products of the dehydration process of HCO_2H may be reacted together via a model of the reversed water–gas shift reaction [34] as follows:

$$CO + H_2O \rightleftharpoons CO_2 + H_2$$

This can explain the relatively higher yield of CO_2 gas (compared with the other products, i.e. CO and HCHO, see figure 4 and table 1).

The rate of the dehydration process was followed through the formation of CO, which was detected by GC analysis. This process is shown to be strongly dependent on the concentration of the acidic sites on the catalyst surface, see figure 4.

(ii) Dehydrogenation process (i.e. $HCO_2H \rightarrow CO_2 + H_2$). The rate of formation of CO_2 (R_{CO_2}), however, showed a similar behavior to that of R_{CO}; the maximum value of R_{CO_2} was attained for the catalyst calcined at 200°C (ca. 242.1 mmol h^{-1} m^{-2}_{cat}). It sharply decreased to less than half of this value at a calcination temperature of 300°C (ca. 108.4 mmol h^{-1} m^{-2}_{cat}). Above 300°C, there was another gradual decrease in the values of R_{CO_2}, see figure 4. Therefore, the rate of formation of CO_2 (R_{CO_2}) is identical with the behavior of both %conversion and S_{BET} of these catalysts, see figure 4 and table 1. In addition, it is also similar to the change in the basicity values Φ of these calcined catalysts, except for the sample calcined at 200°C. The production of CO_2 (R_{CO_2}) may, also, depend on the surface area of the catalyst samples, see table 1. The number of Fe interstitials and oxygen vacancies are appreciably diminished [35] as a result of the decrease in S_{BET} as the calcination temperature increases. Therefore, the activity of the catalysts decreased sharply when calcined at $\geqslant$400°C, see table 1 and figure 4.

(iii) Reduction process (i.e. $HCO_2H + H_2 \rightarrow HCHO + H_2O$). The third product was detected by GC and was identified as formaldehyde. An injected authentic sample of pure formaldehyde, under the same experimental conditions, gave a peak at the same retention time. It is worth noting that no hydrogen gas was detected by GC analysis. XRD analysis has identified the catalyst samples as α-Fe_2O_3 with no diffraction lines attributed to Fe_3O_4 or metallic Fe. Therefore, the hydrogen gas produced from the dehydrogenation of formic acid (i.e. $HCO_2H \rightarrow CO_2 + H_2$) is being used to reduce another molecule of the acid to yield formaldehyde (i.e. $HCO_2H + H_2 \rightarrow HCHO + H_2O$). The rate of formation of formaldehyde (R_{HCHO}) shows a different behavior from that exhibited by both R_{CO} and R_{CO_2}. It was found that R_{HCHO} attains its maximum value (i.e. 36.4 mmol h^{-1} m^{-2}_{cat}) for the catalyst calcined at 300°C. Then, it steadily decreased with increasing calcination temperature reaching 17.1 mmol h^{-1} m^{-2}_{cat} for the catalyst calcined at 600°C. It is clear from figure 4 that the change in R_{HCHO} is consistent with the basicity values Φ of these catalysts. This means that the basicity is favoring deoxygenation to yield formaldehyde.

Formaldehyde was not reported before to result from the decomposition of formic acid. Recently, however, the production of aldehyde by reduction of aliphatic carboxylic acid (e.g. acetic acid) on α-Fe_2O_3 catalysts has been reported by Grootendorst et al. [4]. The production of formaldehyde, in this study, is found to depend on the concentration of the Brønsted basic sites, see figure 4, where the highly basic catalyst, calcined at 300°C, was shown to be the most active catalyst in the production of formaldehyde.

4. Conclusion

The present study showed that three chemical processes took place during the catalytic decomposition, in the gas phase, of formic acid (i.e. dehydration, dehydro-

genation and reduction). Because the basicity (Φ) of our α-Fe_2O_3 samples was relatively higher than their acidity (Ψ), the dehydrogenation process of HCO_2H (i.e. $HCO_2H \rightarrow CO_2 + H_2$) over these catalysts was the predominant process. Therefore, the %selectivity of CO ($\%S_{CO}$) was always less than the %selectivity of CO_2 ($\%S_{CO_2}$), see table 1. This is attributed to the fact that the dehydrogenation process is catalyzed by basic sites [36,37].

The absence of hydrogen as a gaseous product (i.e. in the dehydrogenation process of formic acid) together with the formation of formaldehyde suggested a selective reduction step where hydrogen gas expected to result from the dehydrogenation process is being used up in reducing another molecule of formic acid. This can be explained as follows:

$$HCO_2H \xrightarrow{(\alpha\text{-}Fe_2O_3/200^\circ C)} CO_2 + H_2$$

$$HCO_2H + H_2 \xrightarrow{(\alpha\text{-}Fe_2O_3/200^\circ C)} HCHO + H_2O$$

$$2HCO_2H \xrightarrow{(\alpha\text{-}Fe_2O_3/200^\circ C)} HCHO + CO_2 + H_2O$$

References

[1] G.M. Schwab, Disc. Faraday Soc. 8 (1950) 166.
[2] J. Fahrenfort, L.L. Van Reyen and W.H.M. Sachtler, in: *The Mechanism of Heterogeneous Catalysis*, ed. J.H. de Boer (Elsevier, Amsterdam, 1960) p. 23.
[3] P. Mars, in: *The Mechanism of Heterogeneous Catalysis*, ed. J.H. de Boer (Elsevier, Amsterdam, 1960) p. 49.
[4] E.J. Grootendorst, R. Pestman, R.M. Koster and V. Ponec, J. Catal. 148 (1994) 261.
[5] R. Pestman, R.M. Koster and V. Ponec, Recl. Trav. Chim. Pays-Bas 113 (1994) 426.
[6] M. Ai, J. Catal. 50 (1977) 291.
[7] G. Patermarakis and C. Pavlidou, J. Catal. 147 (1994) 140.
[8] R.B. King, A.D. King Jr. and N.K. Bhattacharyya, Transition Met. Chem. 20 (1995) 321.
[9] S. Haq, J.G. Love, H.E. Sanders and D.A. King, Surf. Sci. 325 (1995) 230.
[10] B.A. Sexton and R.J. Madix, Surf. Sci. 105 (1981) 177.
[11] M. Chtaib, P.A. Thiry, J.J. Pireaux, J.P. Delrue and R. Caudano, Surf. Sci. 162 (1985) 245.
[12] Y. Matsuoka, M. Niwa and Y. Murakami, J. Phys. Chem. 94 (1990) 1477.
[13] J. Kiki, M. Asanuma, Y. Tachibana and T. Shikada, J. Chem. Soc. Chem. Commun. (1994) 691.
[14] A. Kool and F. Riesenfeld, in: *Gas Purification*, 3rd Ed. (Gulf Publishing Company Book Division, Houston, 1979) p. 381.
[15] Y. Tamaura and K. Nishizawa, Energy Convers. Manage. 33 (1992) 573.
[16] H.M. Fortuin, A.J.H.M. Kock and J.W. Geus, J. Catal. 96 (1985) 261.
[17] P. Deygas, C. Goutaudier, F. Guenard and R. Abraham, Compt. Rend. Acad. Sci. Paris, t.321, ser. IIb (1995) 337.
[18] S.A. Halawy and M.A. Mohamed, Collect. Czech. Chem. Commun. 59 (1994) 2253.
[19] P.A. Chemavskii, V.V. Kiselev and V.V. Lunin, Zh. Fiz. Khim. 66 (1992) 2717.
[20] G.C. Bond, S. Flamerz and L.van Wijk, Catal. Today 1 (1987) 229.
[21] S.A. Halawy and M.A. Mohamed, J. Mol. Catal. A 98 (1995) 63.
[22] M.A. Makarova, E.A. Paukshtis, J.M. Thomas, C. Williams and K.I. Zamaraev, J. Catal. 149 (1994) 36.
[23] C.T. Fishel and R.J. Davis, Catal. Lett. 25 (1994) 87.
[24] G.C. Bond, S.A. Halawy, K.M. Abd El-Salaam, E.A. Hassan and H.M. Ragih, J. Chem. Tech. Biotechnol. 59 (1994) 181.
[25] S.A. Halawy, M.A. Mohamed and S.F. Abd El-Hafez, J. Mol. Catal. 94 (1994) 191.
[26] C. Duval, Anal. Chim. Acta 20 (1959) 263.
[27] R.C. Weast, ed., *Handbook of Chemistry and Physics*, 62nd Ed. (CRC Press, Boca Raton, 1982) p. B 109.
[28] E.E. Unmuth, L.H. Schwartz and J.B. Butt, J. Catal. 63 (1980) 404.
[29] M.V.C. Sastri, R.P. Viswanath and B. Viswanathan, Int. J. Hydrogen Energy 7 (1982) 951.
[30] R. Brown, M.E. Cooper and D.A. Whan, Appl. Catal. 3 (1982) 177.
[31] F. Gazzarini and G. Lanzavecchia, *Proc. 6th Int. Symp. on Reactivity of Solids*, Schenectady, NY, August 1968.
[32] C.P. Bezouhanova and M.A. Al-Zihari, Catal. Lett. 11 (1991) 245.
[33] S.S. Al-Shihry and S.A. Halawy, J. Mol. Catal. A 113 (1996) 479.
[34] L.Lloyd, D.E. Ridler and M.V. Twigg, in: *Catalyst Handbook*, 2nd Ed., ed. M.V. Twigg (Wolfe, London, 1989) p. 283.
[35] K.H. Kim, H.S. Han and J.S. Chol, J. Phys. Chem. 83 (1979) 1286.
[36] M. Adachi, K. Kishi, T. Imanaka and S. Teranishi, Bull. Chem. Soc. Jpn. 40 (1967) 1290.
[37] A. Eucken, Naturwissenschaften 36 (1994) 48.